Identification of Acoustic Emission Source and Comparative Study on the Diagnosis of a Spur Gearbox

Lokesh. G. Kamde, Suryabhan. A. Patil, Asso. Prof. U. N. Gujar

Department of Mechanical Engineering
P. G. Student from PREC, Loni, Ahmednagar,
P. G. Student from NRI Institute of Technology, Bhopal,
Asso. Professor in PREC, Loni, Ahmednagar.
Email: lokesh_kamde@yahoo.com
suryabhan.patil28@gmail.com
uttamdasgujar@yahoo.in

Abstract—Manufacturing industry drives the world. Every manufacturing industry is having number of machines and gearboxes. These are used for power transmission, speed reduction and torque amplification and vice versa. Any defect induced in gear may costs high at the time of failure. For that, early prediction of breakage of gear tooth is essential to avoid stoppage of that machine to enhance utilization and reduce breakdown and production. This paper highlights details about experimental programme to ascertain and validitate the applicability of acoustic emission to initial gear defect. The general relationship between the monitoring parameters such as vibration, acoustic emission indicators, visual inspection and the gearbox operating conditions such as load, speed and oil film thickness is highlighted in this paper.

Key Words— **Acoustic Emission, gearbox, vibration, spectra.**

I. Introduction

I. *Gears And The Acoustic Emission*

Gears are the most important mechanisms for transmitting power or rotation, which play an important role in many sorts of machineries. Smooth operation and high efficiency of gears are necessary for the normal running of machineries. Therefore, gear damage assessment is an important topic in the field of condition monitoring and fault diagnosis. Typical localized gear damage types include pits, chips, and cracks on gear tooth surface. With such damage existing on gears, the gear tooth meshing will not be as smooth as the normal gear.

Prediction and control of gear vibration become an important concern particularly in automotive, aerospace and power generation industries. One of the most popular applications of gear sets can be found in the vehicles gearbox. The vibration generated at the gear mesh is transmitted to the housing through shafts and bearings [1].

Acoustic Emission is defined as the transient elastic wave generation due to a rapid release of strain energy within or on the surface of a material. These waves are detected at the surface of the body by a suitable sensor. The principal advantage of AE comes from its high sensitivity. Since AE is produced at a microscopic level, it is more sensitive to detection of loss of mechanical integrity as compared to the well established vibration monitoring technique [2].

II. *Application of Acoustic Emission in detecting defects*

It has been seen that many branches of industry uses Acoustic Emission(AE) technology in detecting defects, for example in the machining industry, the Acoustic Emission was used in detecting tool wear , in process industrial machinery Acoustic Emission is used in detecting the defects of rotating elements such as pitting, cracking, scuffing, rubbing and tooth breakage in gears, bearings and shaft-seal rubbing in the rail transportation industry where Acoustic Emission is used in assessing surface integrity of rail track in the liquid transportation industry, it is also used for detecting cavitation and in centrifugal pumps and gas void fraction measurement in piping transportation [3] .

Prediction and control of gear vibration become an important concern particularly in automotive, aerospace and power generation industries. One of the most popular applications of gear sets can be found in the vehicles gearbox.

II. Experimental Set Up

I. *Gear box*

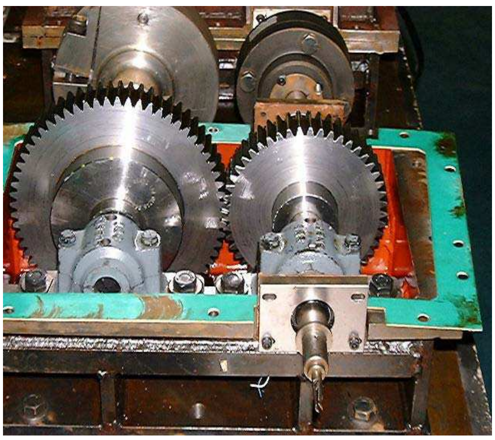

Fig.No.1 Test-rig gearbox set up.

The test-rig used here has two identical oil-bath lubricated gearboxes which are connected in back to back arrangement as shown in "Fig.No.1". The 49 and 65 teeth gear sets were made of 045M15 steel without heat treatment. The gears have a pressure angle of 20°, module of 3 mm and surface roughness between 2-3 µm before operating. Each gearbox has four identical bearings. The method of applying torque is a simple mechanism that allows a pair of coupling flanges to be rotated relative to each other and locked in position. This effectively locks the torque within the gearboxes ensuring that the motor used to drive the test rig only overcome power losses associated with the meshing gears. It is to be note that the 0 Nm condition is not actually '0 Nm' but there will exist a light load at this condition due to the bearing friction and losses or resistance associated with the rubber seals. The motors for driving the gearbox are single speed motors (1.1 kw and 0.55 kw) providing a rotational speed of 745 rpm and 1460 rpm respectively. For this experimental set-up, five torque loadings are used i.e., 0 Nm, 55 Nm, 110 Nm, 183 Nm and 220 Nm [2].

II. Data Acquistion Procedure

Fig.No.2 AE sensor located on pinion.

The AE sensors used here is wide band type sensors with a relative flat response between 100 kHz and 1 MHz (WD model, 'Physical Acoustics Corporation'). An AE sensor was placed on the pinion (49 teeth), as shown in "Fig.No.2". The cable connecting the pinion sensor was fed into the pinion shaft to the pre-amplifier via a slip ring. This allows the AE sensor to be placed as close as possible to the gear teeth. Both the sensors are hold in place with mechanical fixtures. An 'IDM Electronics Ltd' manufactured PH-12 slip ring is used. The slip ring used sliver contact and could accommodate a maximum of 12 channels. The cooling air pressure for the slip ring is 1400 kg/mm^2. Pre-amplification was set at 40dB. The signal output from the preamplifier is connected directly to a commercial data acquisition card. The data acquisition card could provide 10 MHz sampling rate and incorporated 16-bit precision giving a dynamic range of more than 85 dB. Prior to the analog-to-digital converter (ADC), the card uses anti-aliasing filters that can be controlled directly in software. A K-type thermal couple, rated from – 200^0 C to 1378^0 C is used to measure the oil temperature for computation of oil film thickness. The oil bath temperature is measured through an opening on top of the gearbox casing using the specified thermal couple probe. This position for acquiring oil temperatures is adjacent to the gear mesh position as this is the closest position the observer could get access.

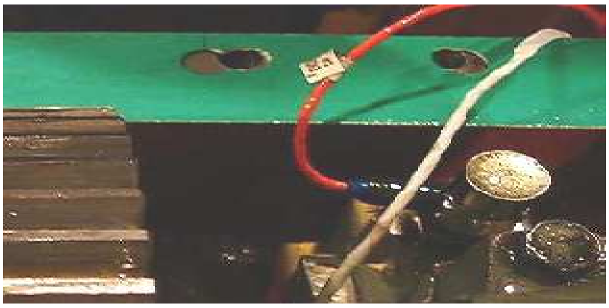

Fig.No.3 Accelerometer located on bearing casing.

The accelerometer as shown in"Fig.No.3" for vibration measurement in this set-up is resonant type sensor with a flat frequency response between 10 Hz and 8000 Hz (Model 236 Isobase accelerometer, 'Endevco Dynamic Instrument Division')[2].The accelerometer is mounted on the base of the pinion bearing casing to capture vibration data of the gearbox. The charge amplifier used is a single channel PE amplifier (Endevco Dynamic Instrument Division, Model 2721B). The accelerometer is connected to a charge amplifier and the signal output from the pre-amplifier is fed to a commercial data acquisition card. Energy, r.m.s and frequency domain information is computed from the raw time-domain data.

III. Test Procedure

Fig.No.4 Seeded large addendum defect.

Before starting an experiment the gearbox is allowed to operate for 15 hours. After that a large addendum defect (extended from the pitch-line) measuring 12 mm along the face width and 3 mm from the pitch-line to the gear tip is seeded on one of the pinion tooth surface as shown in "Fig.No.4". Total five experimental combinations is undertaken: two speed and three load conditions. For each test condition, the gearbox is allowed to run from a cold start for several hours until the oil temperature reached equilibrium, i.e. it reach a temperature that did not change as a function of running time. Equilibrium is observed when oil temperature varied by less than 0.2^0 C for a period of one hour. The oil temperatures and vibration data is taken at 15 minute intervals throughout the duration of the test while AE r.m.s. and energy values is monitored continuously. AE time signatures were got for each test condition after 30 minutes from the start. For analysis of AE data obtained from these experiments, r.m.s and energy were used to provide a comparison and because of the simplicity and proven robustness of these parameters for machine health diagnosis.

IV. *AE fault identification capability*

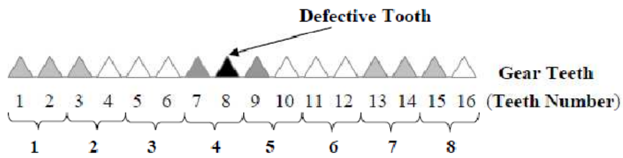

Fig.No.5 Sectioning of gear teeth for analysis.

"Fig.No.5" shows the sectioning of gear teeth for the analysis. For the rotational speeds of 745 and 1460 rpm, the recorded AE time waveform is split into regions representing 2-teeth and 1-tooth. "Fig.No.5" illustrates the case for 2-teeth regions at 745 rpm. The r.m.s. value for each region is calculated for each data set. This is equivalent to '8' and '16' r.m.s values for 2-teeth and 1-tooth data sets respectively. A total of 50 data sets are acquired for each test condition and the r.m.s values shown is averaged for each region over all fifty data sets. The averaging can be accomplish due to the optical triggering system used ensuring that the acquisition system always start at the same rotational position of the gears. It is assumed that this method of grouping the data enhance the possibilities of detecting the seeded defect particularly as the defect had been seeded in the centre of the acquisition window, shown in "Fig.No.5".

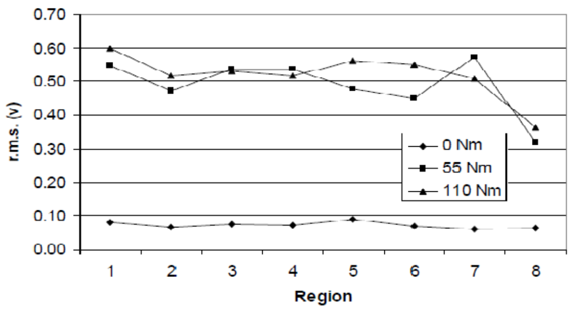

Fig.No.6 r.m.s against loads for 2-teeth analysis at 745 rpm (8 regions).

For the seeded defect simulation at 745 rpm, the r.m.s. values remained random for the three loading conditions, shown in "Fig .No.6".

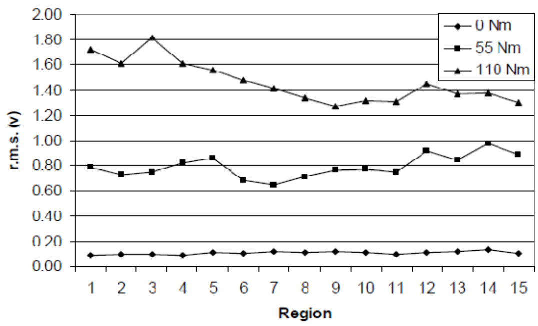

Fig.No.7 r.m.s against loads for 2-teeth analysis at 1460 rpm (15 regions).

The centre region '4', where the seeded defect is introduced, did not exhibit the highest r.m.s. value as expected. The same observations is made for the rotational speed of 1460 rpm, the highest r.m.s. values did not found in the seeded fault region of region '8', shown in "Fig .No.7".

V. *Vibration Analysis*

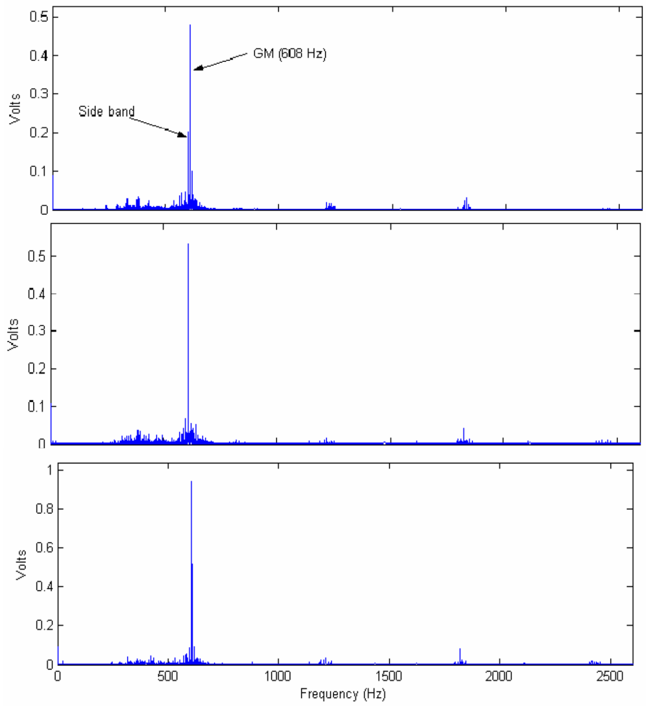

Fig.No.8 Frequency spectra for (a) 0 Nm, (b) 55 Nm and (c) 110 Nm load conditions at 745 rpm.

From the acquired vibration signatures, the r.m.s. and energy value is calculated, and vibration frequency spectrum studied. A sampling rate of 8192 data points per second (8192 Hz) over duration of approximately five seconds (40000 data points), which is approximately equivalent to 61 and 119 revolutions, is used for vibration data acquisition at rotational speeds of 745 and 1460 rpm respectively. For the rotational speed of 745 rpm, all three load conditions exhibited similar frequency content; the highest peaks in the frequency domain occurred at the gear mesh frequency, 608 Hz, and sidebands is observed around this frequency as shown in “Fig .No.8”.

Harmonics of the gear mesh frequency were noted at 1200 Hz, 1800 Hz and 2400 Hz. The peak value at the gear mesh frequency increased from 0.5 to 1.0 g from no-load condition to 110 Nm. As side bands about the gear mesh frequency were seen, as shown in “Fig.No.8”, this is indicative of a defective tooth. Vibration frequency spectra results at 1460 rpm are shown in “Fig.No.8”. A unique observation is that the wide band of frequency response ranging from 0 to 2600 Hz which is not present at the lower speed of 745 rpm . Under no-load condition, the peak value at the gear mesh (GM) frequency of 1200 Hz was 0.03 g. The dominant frequencies in this spectrum were noted to be the sub-harmonics of the gear mesh frequency at 300, 400, 600 and 800 Hz (0.25, 0.33, 0.5 and 0.67 GM). When the load increased to 55 Nm, the dominant frequency was at 400 Hz (0.33 GM). Following an increase in load to 110 Nm, the dominant frequency shifted back to the gear mesh frequency with a peak value of 0.2 g. It is also important to note the strong presence of the second harmonic gear mesh frequency at 2400 Hz.

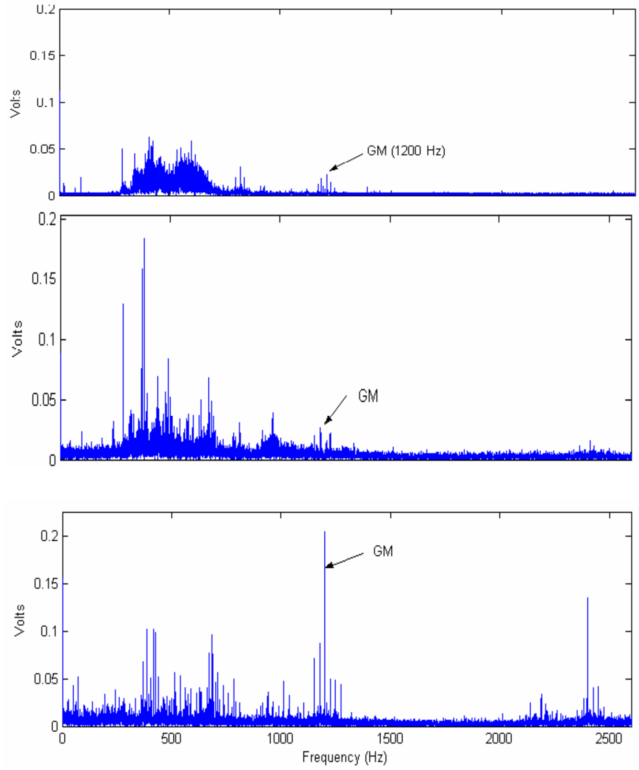

Fig.No.9 Frequency spectra for (a) 0 Nm and (b) 55 Nm and (c) 110 Nm load conditions at 1460 rpm.

More study is undertaken to understand the unique frequency spectra at 1460 rpm. Gears are described as lightly loaded when applied load on the gear is not sufficiently high enough to maintain contact during meshing. The phenomenon usually occurs due to light loads or high loads with large transmission errors (TE). From “Fig.No.9”, the presence of strong harmonics at the gear mesh frequency is evident and the harmonics increases with a reduction in load. Hence, a lightly loaded condition is suspected to exist under certain conditions at 1460 rpm. It is thought confirm to ascertain if the test gears could be considered as lightly loaded. Assuming a Transmission Errors (TE) of 5 µm, which is typical for spur gears , the torques required to maintain the meshing teeth in contact is calculated at 43 Nm and 107 Nm for the pinion and gear respectively, both at a rotational speed of 1460 rpm. Hence, for the 55 Nm test condition, the applied load is lower than the required torque to maintain the meshing teeth in contact, 107 Nm, hence loss of contact is likely to occur, as confirmed earlier. For the 110 Nm test condition, the applied torque is marginally higher than the required torque of 107 Nm. Thus, it is concluded that no contact loss occurred under this situation, which is evident from the differences in the frequency spectra between “Fig.No.9 (c)” and “Fig.No.9 (b)”. Based on the same concept, the required torques for the gear teeth to remain in contact are also computed for the case of 745 rpm; 11 and 28 Nm for the pinion and gear respectively. With the minimum applied torque of 55 Nm, which is higher than the required torque of 28 Nm, the gears will not be lightly loaded. Clearly, vibration analysis is capable of diagnosing the large seeded defect.

VI. Oil Temperature and Film Thickness

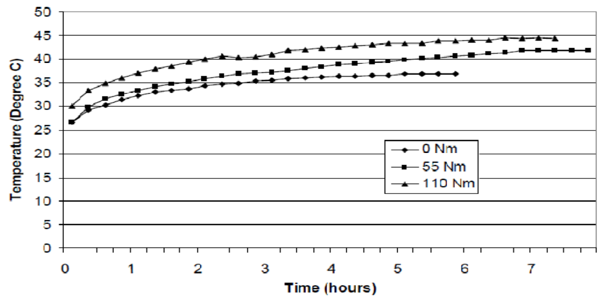

Fig.No.10 The effect of load on oil temperature for speed of 745 rpm.

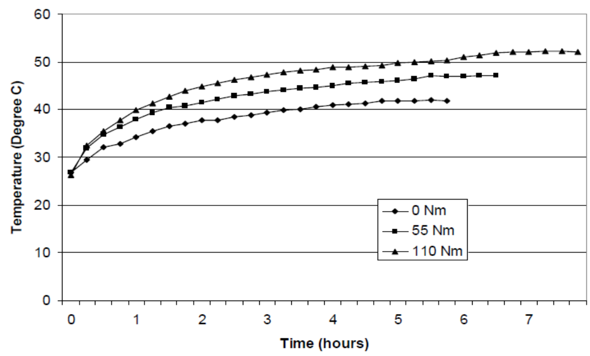

Fig.No.11 The effect of load on oil temperature for speed of 1460 rpm.

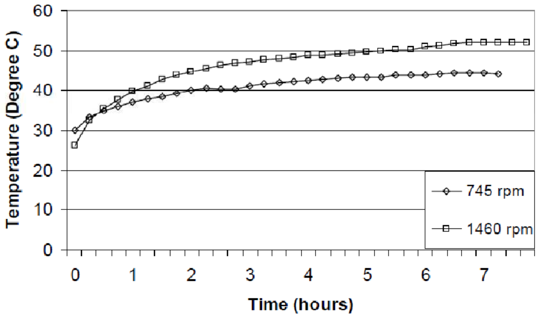

Fig.No.12 The effect of load on oil temperature for load of 110 Nm.

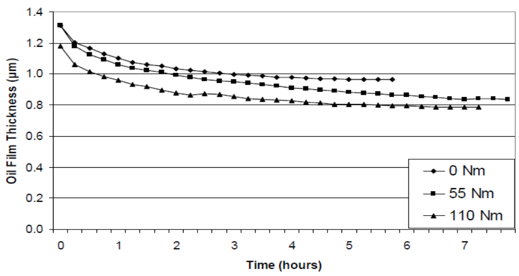

Fig.No.13 The effect of load on oil film thickness for speed of 745 rpm.

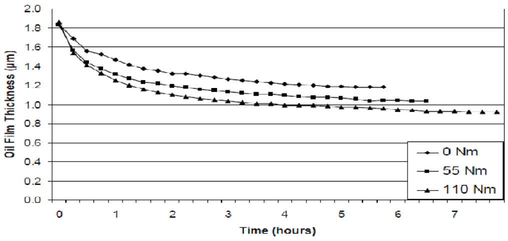

Fig.No.14 The effect of load on oil film thickness for speed of 1460 rpm.

To understand the limitations of the AE technique for defect identification further tests were carried out. This involves measuring the oil temperature of the gearbox sump from a cold start to the operational oil temperature and calculating the oil film thickness between the gears. Results from the six test conditions is plotted to observe the effect of speed and load over the oil temperature and film thickness. For both speeds (745 and 1460 rpm), the operational oil temperatures increased with increased loads and speeds, as shown in "Fig.No.10". to "Fig.No.14".

Results of theoretical oil film thickness are shown in "Fig.No.13". and "Fig.No.14". Based on the surface finish of 1.75 µm, the results shows asperity contact for all test condition.

Possible sources of errors for the oil film thickness calculation are:

• The assumption of constant density, as oil density will change with temperature and affect on oil film thickness.

• The measurement of oil temperatures. It is not possible to measure the oil temperature in the gear mesh due to obviously access problems. Hence, the oil temperatures were taken at the oil bath location as near to the gear mesh as possible. The oil bath temperatures recorded will certainly be lower than the actual oil temperatures.

VII. Constant Temperature Tests

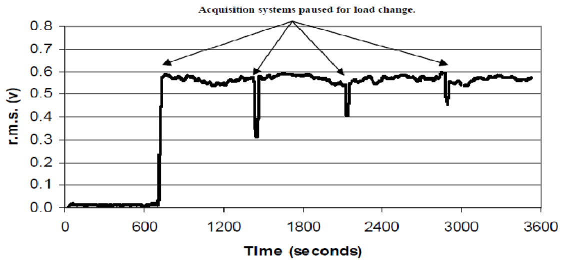

Fig.No.15 AE r.m.s. remained constant with increased load at 745 rpm

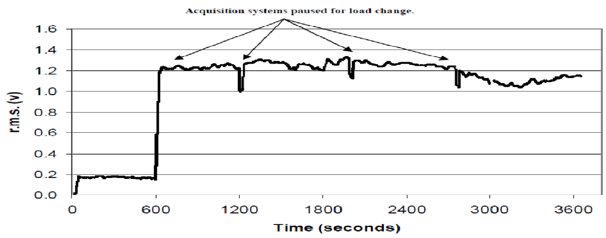

Fig.No. 16 AE r.m.s. remained constant with increased load at 1460 rpm

The three main factors affecting the AE signal in these experiments are namely; speed of rotation, applied torque (load) and the oil temperature. In order to further examine the speed and load effect on AE signal for this back-to-back gearbox arrangement, constant temperature tests were taken. Since the oil temperatures were kept constant, the oil viscosity and film thickness remains constant during the experiment.

The gearbox was run at 745 rpm with a load of 220 Nm for 5 hours at which time the oil temperature stabilised at 42.7^0C. The gearbox is brought to a stop and adjusted to no load condition. The gearbox is re-started and run for 10 minutes while continuous AE data in the form of r.m.s and energy is recorded. The gearbox is again brought to a stop and adjusted to the next load condition. Every load condition was run for a 10 minute interval while the continuous AE r.m.s. and energy data is taken. The time taken to strip the rig and set the new torque level is approximately three minutes. During this period the acquisition system is paused. A total of 5 load conditions; 0, 55, 110, 183 and 220 Nm, is tested. In these tests, the average oil temperature was at 42.4^0C with a maximum temperature difference of 1.8^0C to minimise the temperature effect.

At the rotational speed of 745 rpm, the continuous AE r.m.s. values were plotted for the 5 loading conditions and shown in “Fig.No.15”. It is observed that the AE r.m.s remains constant at 0.58 volts with increasing loads. For the 1460 rpm test condition, the same test procedures were done, the oil temperature stabilised at 51.8^{0}C. The mean oil temperature is kept at 50.8^{0}C with a maximum temperature difference of 3.5^{0}C to ensure constant temperature condition. The AE r.m.s. is plotted against the five loading conditions, as shown in “Fig.No.16”. Similar trend is observed when compared to the lower running speed condition. With increasing load, the AE r.m.s remained constant at 1, 2 volts. From the above results, it is concluded that at constant oil temperature, the applied load on the gear system had negligible effect on AE r.m.s. On the other hand, speed had a more significant effect on the AE indicators. By doubling the rotational speed from 745 rpm to 1460 rpm, the AE r.m.s increased from 0.58 to 1.2 volts by a factor of 2. Between the two rotational speeds, there is a temperature difference of 8.4^{0}C.

The AE r.m.s increased with decreasing viscosity. Hence, for this experiment, the increase in the AE parameters at 1460 rpm is partially due to the higher oil temperature at the higher rotational speed.

VIII. Friction and asperity contacts

During the gear mesh; sliding, rolling or a combination of both will occur. As the gear teeth surfaces are limited to manufacturing capabilities (approximately 0.4μm) asperity contacts will occur during meshing on almost all gears, particularly as the calculated oil film thickness in this case is less than the composite roughness.

During the test, it is noted that transient shock pulses during gear mesh at the gear mesh frequency. It is concluded that these shocks were attributed to asperity contact. While a single asperity model is presented as the probable cause of the shocks, such scenario in practice is limited, multiple contacts is seen.

However, it is seen that based on an asperity width of 5μm and sliding and rolling velocities of the order of 500mm/s, the raise time for such a transient event is 10μs. It must be noted that the sensors use has a natural frequency of 50 kHz and is outside the range of AE.

The relationship between sliding and rolling friction has been found. It is seen that while the rolling friction traction is independent of load the sliding friction traction is influenced by the lubricant viscosity and load. Moreover, it is seen that increasing rolling speed resulted in a reduction of friction traction for a fixed load and lubricant viscosity. Following observations seen here is of relatively constant r.m.s. values at a fixed speed and temperature irrespective of load, some resemblance to the phenomena of rolling friction, and elasto hydrodynamic lubrication.

It is observed that the oil viscosity effects on AE and wear in lubricated sliding contacts. Several observations were seen including an increase in AE r.m.s with decreasing viscosity and increased rotational speed, but more importantly, the source of AE under lubricated sliding conditions is attributed to asperity contact. It is studied that the basic mechanism for AE generation was the elastic deformation of the material at asperity contacts. This deformation is mated by increased rates (sliding speed), contact forces and lubrication. The range of surface finish for the materials highlighted was from 1 to 4μm; comparable with the gears tested.

All the above comments provides strong evidence to suggest that the source of AE during gear mesh is attributed to asperity contact.

III. Conclusion

The general relationships between monitoring parameters such as vibration and AE indicators and the gearbox operating conditions such as load, speed and oil film thickness has shown in this paper. It is important to note that various indicators within a monitoring technique must be used simultaneously in order to establish and explain the phenomena observed. The most ideal situation is to use various techniques to monitor the gearbox health status at the same time. This paper has shown that gear defect detection with AE is little difficult. Seeded defect identification with AE r.m.s. and energy were not satisfactory. The influence of oil temperature on AE activity has shown as the primary reason for this limitation. It is concluded that the source of AE mechanism that produced the gear mesh bursts was from asperities contact. Vibration measurements can tell us about the condition of a gearbox, if properly done. Other physical parameters besides vibrations can be helpful. Trending of data should be helpful but only if the data being trended is collected consistently. Methods of mounting of transducers such as accelerometers used for measuring high frequency data are important. Repeatability of data collection is the most important consideration in choosing a mounting method in this case.

References

[1] Shawki Abouel , seoud, Ibrahim Ahmed and Mohamed Khalil , “An Experimental Study on the Diagnostic Capability of Vibration Analysis for Wind Turbine Planetary Gearbox evaluation through multibody TE-based simulation.” , International Journal of Modern Engineering Research (IJMER) , Vol.2, Issue.3, pp-667-675ISSN:2249-6645, May-June2012.

[2] Chee Keong Tan and David Mba, “Identification of the Acoustic Emission source during a comparative study on diagnosis of a spur gearbox, ” Tribology International ,Volume 38,Issue 5,Pages 469-480,5 May 2005.

[3] Shuib Husin, D.Mba and R.I. Raja Hamzah, “Viability of the Application of Acoustic Emission (AE) Technology for the Process and Management of Maintenance in Industries: Defect Detection, On-Line Condition Monitoring, Diagnostic and Prognostic Tools”, Proceedings of the International Multi Conference of Engineers and Computer Scientists 2010 Vol III,IMECS 2010, Hong Kong, 17-19 March 2010.

[4] Sameh M. Metwalley, Nabil Hammad, Shawki A. Abouel-Seoud, "Vehicle gearbox fault diagnosis using noise measurements", International Journal Of Energy And Environment, Volume 2, Issue 2, pp.357-366, Feb 2011.
[5] Ghalib R. Ibrahimand A. Albarbar, "Gearbox Fault Features Extraction Using Vibration Measurements and Novel Adaptive Filtering Scheme", Advances in Acoustics and Vibration Volume 2012, Article ID 283535, 7 pages,11 June 2012.
[6] G. Dalpiaz, A. Rivola and R. Rubini, "Gear Fault Monitoring: Comparison of Vibration Analysis Techniques", CNR - Italian National Research Council, Feb 2008.
[7] Pavel Mazal, Libor Nohal, Filip Hort, Vacav Koula, "Possibilities of the damage diagnosis of gearboxes and bearings with acoustic emissions method", 18th World Conference on Non destructive testing, Durban, South Africa, 16-20 April 2012.
[8] Brian C. Howes, "A Gearbox Vibration - Fact or Fiction , " Beta Machinery Analysis Ltd. Calgary AB, Canada, T3C 0J7, Oct 2001.
[9] G. Dalpiaz, A. Rivola And R. Rubini, "Effectiveness And Sensitivity Of Vibration Processing Techniques For Local Fault Detection In Gears", Mechanical Systems and Signal Processing (2000) 14(3), 387}412, May 2000.
[10] Wenyi Wang and Albert K.Wong, "Autoregressive Model-Based Gear Fault Diagnosis,"Transactions of the ASME, Vol.124, April 2000.

